High-order Sliding Mode Control of a Bioreactor Model through Non-Commensurate Fractional Equations

Fatemeh Saeedizadeh[1*], Naser Pariz[2], Seyyed Abed Hosseini[3]
1- Department of Electrical Engineering, Mashhad Branch, Islamic Azad University, Mashhad, Iran.
Email: f.saeedizadeh@yahoo.com (Corresponding Author)
2- Department of Electrical Engineering, Ferdowsi University of Mashhad, Mashhad, Iran.
Email: n-pariz@um.ac.ir
3- Research Center of Biomedical Engineering, Mashhad Branch, Islamic Azad University, Mashhad, Iran.
Email: Hosseyni@mshdiau.ac.ir

Received: July 2017 Revised: September 2017 Accepted: January 2018

ABSTRACT:
A higher-order sliding approach to control a bioreactor model is proposed by non-commensurate fractional equations. According to existing conditions and chattering reduction, a high-order sliding mode approach has been chosen to design the controller. A mathematical problem is a barrier to use the high-order sliding mode approach for fractional order systems. The contribution of the paper is to choose proper sliding surfaces. High-order sliding mode controllers have been taken in accordance with the structure of integer order system. Thus, in order for the system to apply more precise calculations, fractional systems should somehow turn to integer order. The sliding surfaces have been selected so appropriately that we can benefit from the structure of integer order controllers for fractional order system. The sliding surface in both controllers has also been the same so as to provide conditions for comparison. The model outputs are reached the desired values using two controllers. Finally, the comparison in simulations indicates that the proposed approach has a great impact on chattering reduction.

KEYWORDS: Bioreactor, Non-commensurate fractional equations, Chattering reduction, High- order sliding mode.

1. INTRODUCTION

So far, many researchers from different fields of sciences have been tended to work on fractional calculus, for practical systems [1-4]. Fractional calculus is expanded in modeling the phenomena and systems behavior [5-10]. Some of these practical systems or natural phenomena might be described more precisely by fractional calculus, that is why discovering ways in a much better recognition of phenomena is counted as influential. In control science, researchers have paid attention to fractional order model of systems and fractional-order controllers. Fractional-order controllers can control a fractional-order or an integer-order system [11-17]. Moreover, integer-order controllers have been applied to control fractional-order ones [18-21].

High-order sliding mode controllers have been applied by Levant [22-24]. He simulated the model of a vehicle tracking a trajectory, to show the efficiency of the high-order sliding. Shtessel et al. in 2014 [25] explained mathematical basics of high-order sliding mode controllers, then they introduced two classes of such controllers. Other researchers have used the above approach to reduce chattering [26-33].

Rhif in 2012 [26] used high-order sliding mode to control a naval weapon actuator. The form of sliding surface was based on lead-lag controller. His results indicated a desirable performance of the mentioned method. Girin et al. in 2009 [27] controlled an electro-pneumatic actuator by high-order sliding mode controller. The electro-pneumatic actuator tracks a desired value by two controllers. Comparing the performance of two controllers indicated that one with high-order sliding mode has higher efficiency. Liu and Han in 2014 [28] designed a high-order sliding mode controller for a nonlinear class of multi-input multi-output (MIMO) systems. Some other researchers have also implemented the mentioned controller for other systems successfully [29-33]. They have mainly shown the efficiency of controllers with high-order sliding mode by comparing to other controllers. The previous researchers considered integer order systems. Pisano et al. in 2010 [33] applied second-order sliding mode so as to stabilize a class of fractional-order systems. The state-space model of the system is linear and includes commensurate orders. Their results reached the desired performance by a Lyapunov candidate function.

Unlike the reviewed papers, this paper presents a fractional high-order sliding mode controller for a fractional nonlinear problem.

In the current paper an uncertain model of a bioreactor is considered. According to bounded uncertainty in parameters of the model, a sliding mode approach is a good choice. The most important issue of the method is chattering on which there have been a lot of attempts made in order to get it removed. A high-order sliding mode has been used to reduce chattering. Derivative orders of the bioreactor model are not the same. The appropriate high-order controller must be chosen with respect to the relative degree of the system. The structure of these controllers was calculated for integer order systems [25]. In this paper, a problem caused by fractional orders is ignored by defining suitable sliding surfaces.

The correct estimation of fractional order model is not important here; so the selected model is obtained simply by using fractional order derivative instead of integer order derivative. Orders are selected to obtain a general solution; so there will be no specific way to solve the problem. Assuming the orders to be taken correctly, designing controllers can be started. The goal is to show the solution for nonlinear systems with non-commensurate orders.

This paper is organized as follows: In section 2 mathematical preliminaries of fractional calculus is described. In Section 3, first, the problem description is discussed; then, standard sliding mode and high-order sliding mode strategies are designed separately. In Section 4, results and simulations are expressed. Finally, discussions and conclusions are presented in Section 5.

2. MATHEMATICAL PRELIMINARIES

Definitions and properties that have been used are briefly discussed in this section. Fractional order derivative has various definitions. To describe practical systems, Caputo definition is normally used because initial conditions are measurable in the definition of Caputo and it has also a physical concept.

Definition 1: The derivative of the function $f(t)$ with Riemann-Liouville ($_R$) definition is shown in (1). Where α is the order and $m-1<\alpha<m$, $m\in N$ [2].

$$ {}^{R}D^{\alpha} f(t) \overset{\Delta}{=} \frac{d^m}{dt^m}\left[\frac{1}{\Gamma(m-\alpha)}\int_0^t \frac{f(\tau)}{(t-\tau)^{\alpha-m+1}} d\tau\right] \quad (1) $$

the symbol D denotes the fractional derivative operator and $\Gamma(.)$ denotes the Gamma function.

Definition 2: Caputo (C) defined the derivative of the function $f(t)$ as (2):

$$ {}^{C}D^{\alpha} f(t) \overset{\Delta}{=} \left[\frac{1}{\Gamma(m-\alpha)}\int_0^t \frac{f^m(\tau)}{(t-\tau)^{\alpha-m+1}} d\tau\right] \quad (2) $$

Property 1: Definitions of Riemann-Liouville and Caputo derivative are exchangeable through (3).

$$ {}^{R}D^{\alpha} f(t) = {}^{C}D^{\alpha} f(t) + \sum_{k=0}^{m-1} \frac{t^{k-\alpha}}{\Gamma(k-\alpha+1)} f^{(k)}(0^+) \quad (3) $$

Property 2: Integer order derivative can be taken from the definitions of Riemann-Liouville and Caputo are as relations (4) and (5).

$$ \frac{d^m}{dt^m} {}^{R}D^{\alpha} f(t) = {}^{R}D^{m+\alpha} f(t) \quad (4) $$

$$ {}^{C}D^{\alpha}\left(\frac{d^m}{dt^m} f(t)\right) = {}^{C}D^{m+\alpha} f(t) \quad (5) $$

3. DESIGNING CONTROLLERS

3.1. Introduction to bioreactor

Bioreactors are engineered plants treating industrial wastewater by a biochemical process. A biochemical process is carried out by aerobic or anaerobic microorganisms. The high sensitivity of microorganisms and the necessity of a certain concentration will definitely bring up a need for a system with an ability to control. A desired environmental bioreactor feeds the process with organic materials so as to make a proper growth; meanwhile, the Intended concentration is under control.

Some of these bioreactors use “chemical oxidation” to treat wastewater. The main purpose of the process is to reduce the concentration of chemical particles in order to achieve the standardized quantity defined by the Environmental Protection Agency (EPA). Generally, there are different ways to refine the industrial wastewater, but “active sludge” is one of the most popular ways. The block diagram of refining wastewater through active sludge is presented in Fig. 1.

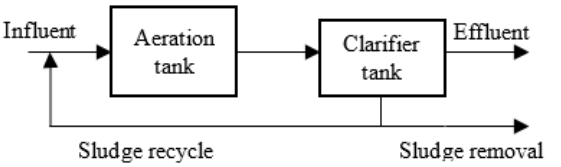

Fig. 1. Active sludge process.

Fig. 1 indicates a usual biologically wastewater refining. The organic material is decomposed by biological oxidation using the existing microorganisms in the aeration tank. Refining process then takes place in terms of remaining suspended sludge in aeration tissue. Suspended materials include organic and inorganic particles in which some of those organic particles can get decomposed by hydrolysis. The rest of particles constitute an inert mass. Decomposing tank separates

suspended material from refined water as a secondary refiner. Some amount of sludge in the form of sediment is refined and the extra gets out of the device. The output wastewater can be released to the environment if having environmental standards. A mathematical model of biologically wastewater refining process discussed in this article is in terms of a Nejjari's model [34] expressed in (6). According to the measured initial conditions in laboratory, The Caputo's definition is used to describe the system.

$$
\begin{aligned}
&{}^{C}D^{\alpha_1}X = (\mu_{\max}\frac{S}{S+K_S}\times\frac{DO}{DO+K_{DO}}-\mu_s)X\\
&-D(1+r)X - rDX_r\\
&{}^{C}D^{\alpha_2}S = -\frac{1}{Y}(\mu_{\max}\frac{S}{S+K_S}\times\frac{DO}{DO+K_{DO}}-\mu_s)X\\
&-D(1+r)S + DS_{in} + dis1(t)\\
&{}^{C}D^{\alpha_3}DO = -\frac{10^3(1-Y)}{Y}(\mu_{\max}\frac{S}{S+K_S}\times\frac{DO}{DO+K_{DO}}-\mu_s)X\\
&-D(1+r)DO + 60\alpha W(DO_{Sat}-DO) + DO_{in}D + dis2(t)\\
&{}^{C}D^{\alpha_4}X_r = D_S X(t) + rD_S(X(t)-X_r(t)) - \beta D_S X_r(t)\\
&-D_S(1-\beta)\eta X_r(t)
\end{aligned}
\tag{6}
$$

The growth rate of microorganisms ($\mu(t)$) depends on system state variables according to (7).

$$\mu(t) = \mu_{\max}\frac{S}{K_S+S}\times\frac{DO}{K_{DO}+DO}-\mu_s \tag{7}$$

Where X indicates the sludge (biomass); X_r shows recycled sludge; S is organic substance concentration (substrate), and DO signifies dissolved oxygen.

Equations of system output variables are subjected to bounded disturbances of $dis1(t) = 0.01\cos(\pi t), dis2(t) = 0.1\sin(2\pi t)$.

Moreover, few internal variables are not definite which we can see in Table 1. Other input parameters of the process are discussed in Table 2.

$u = [D \quad W]^T$ and $y = [S \quad DO]^T$ are the inputs and outputs of the system, respectively.

The purpose is to keep the concentration of materials fed (S) on 0.1 $g.L^{-1}$ and to keep the dilution oxygen (DO) on 2 $mg.L^{-1}$ by controlling dilution rate of the material (D) and an aeration rate of the process (W).

Table 1. Uncertain parameter in model.

Parameter	Definition	Value	Typical value	Unit
$\mu_{\max}$	Maximum specific growth rate	0.11	0.12-0.55	h^{-1}
K_{DO}	Saturation constant	0.20	0.01-0.5	$mg.L^{-1}$
K_S	Saturation constant	0.18	0.1-0.18	$g.L^{-1}$
Y	Biomass yield factor	0.67	0.46-0.69	-
μ_S	Decay coefficient for biomass	0.02	0.002-0.07	h^{-1}

Table 2. Constant parameters of input.

Parameter	Definition	Value	Unit
S_{in}	Substrate concentrations in the influent	1.2	$g.L^{-1}$
DO_{in}	Dissolved oxygen concentrations in the influent	2	$mg.L^{-1}$
D_S	Dilution of sludge compartment	0.017	h^{-1}
DO_{sat}	Dissolved oxygen saturation concentration	8	$mg.L^{-1}$
α	Oxygen transfer rate	0.0033	-
R	Ratio of recycled flow of the influent	1.00	-
β, r	Ratio of waste flow of the influent	0.20	-
η	Parameter of the clarifier model	8	-

3.2. Standard sliding mode

Standard sliding mode controller is considered by (8) to reach the surface in a certain time.

$$u_{SMC} = u^{eq} - Ksign(S(t)) \tag{8}$$

where u_{SMC} is standard sliding mode controller, u^{eq} is a nominal controller, and $S(t)$ is the sliding surface. If the nominal quantity of the model is $\hat{\Theta}$ and its uncertain amount is Θ and their differences are bounded by a known function A as ($\left|\Theta-\hat{\Theta}\right| \le A$), then by choosing K as (9), it can be guaranteed that trajectories reach to sliding surfaces in a finite time.

$$K = A + \varepsilon \tag{9}$$

Where ε is an affirmative optional quantity. Proving a finite reaching time by (8) is demonstrated in the source [35].

According to the problem controlling purpose, tracking error in outputs is shown in (10). So a proper sliding surface can be recommended as that in (11).

$$\begin{aligned} S - 0.1 &= e_1 \\ DO - 2 &= e_2 \end{aligned} \tag{10}$$

$$\begin{aligned} S_S &= D^{-1+1\times\alpha_2}(e_1) + c_1 D^{-1+0\times\alpha_2}(e_1) \\ S_{DO} &= D^{-1+1\times\alpha_3}(e_2) + c_2 D^{-1+0\times\alpha_3}(e_2) \end{aligned} \tag{11}$$

Where e_1 and e_2 are the tracking errors of the outputs. The reason of choosing fractional order for sliding surface in calculating the nominal controller is that defined states in dynamic equations should appear to provide an implementing condition. A Riemann-Liouville definition has been used to write the sliding surfaces; so we can get derivatives from equation (4) to achieve nominal controller. Proving the stability of these sliding surfaces is able to be discussed through writing Hurwitz polynomial. Hurwitz polynomial of sliding surfaces in (11) is written through (12). The Hurwitz polynomial is calculated by the Laplace transform of the sliding surface.

$$\begin{aligned} \mathcal{L}(S_S) = [s^{\alpha_2} + c_1], s^{\alpha_2} = \lambda_1 \\ \rightarrow P(\lambda_1) = [\lambda_1^1 + c_1\lambda_1^0] \\ \mathcal{L}(S_{DO}) = [s^{\alpha_3} + c_2], s^{\alpha_3} = \lambda_2 \\ \rightarrow P(\lambda_2) = [\lambda_2^1 + c_2\lambda_2^0] \end{aligned} \tag{12}$$

Stability condition of sliding surfaces is satisfied if the roots of Hurwitz polynomial are held in (13).

$$\alpha\frac{\pi}{2} < \arg(roots(P(\lambda)) \le \pi \tag{13}$$

Where c_1 and c_2 are constants that determine the roots of the Hurwitz polynomial. The condition (13) is satisfied by taking $c_1 = c_2 = 1$; therefore sliding surfaces will become stable.

The system model in (6) is considered with parameters and initial quantities in Tables 1 and 2. Derivative orders are also considered as $\alpha_1 = 0.7, \alpha_2 = 0.8, \alpha_3 = 0.5$ and $\alpha_4 = 0.4$.

The model including values of Table 1 and 2, is seen in (14).

$$\begin{aligned} {}^{C}D^{0.7}X &= (0.11\times\frac{S}{S+0.18}\times\frac{DO}{DO+0.2} - 0.02)X \\ &- 2DX - DX_r \\ {}^{C}D^{0.8}S &= -\frac{1}{0.67}(0.11\times\frac{S}{S+0.18}\times\frac{DO}{DO+0.2} - 0.02)X \\ &- 2DS + 1.2D + dis1(t) \\ {}^{C}D^{0.5}DO &= (-54.1791\frac{S}{S+0.18}\times\frac{DO}{DO+0.2} + 9.8507)X \\ &- 2D\times DO + 0.1980\times W(8-DO) + 2D + dis2(t) \\ {}^{C}D^{0.4}X_r &= (0.0340X - 0.03X_r)D \end{aligned} \tag{14}$$

To calculate nominal controllers, the error dynamics must be obtained. Through the relations in (14), the error dynamics are as in (15).

$$\begin{aligned} &{}^{C}D^{0.8}S - {}^{C}D^{0.8}0.1 = {}^{C}D^{0.8}e_1 \\ &= -\frac{1}{0.67}(0.11\times\frac{S}{S+0.18}\times\frac{DO}{DO+0.2} - 0.02)X - 2DS \\ &+1.2D - {}^{C}D^{0.8}0.1, \\ &{}^{C}D^{0.5}DO - {}^{C}D^{0.5}2 = {}^{C}D^{0.5}e_2 \\ &= (-54.1791\frac{S}{S+0.18}\times\frac{DO}{DO+0.2} + 9.8507)X \\ &-2D\times DO + 0.1980\times W(8-DO) \\ &+2D - {}^{C}D^{0.5}2 \end{aligned} \tag{15}$$

A nominal controller is calculated through sliding surfaces in (11) and applying (4).

$$\begin{aligned} \dot{S}_S &= {}^{R}D^{\alpha_2}(S-0.1) + (S-0.1) \\ \dot{S}_{DO} &= {}^{R}D^{\alpha_3}(DO-2) + (DO-2) \end{aligned} \tag{16}$$

In order to design a nominal controller and according to the fact that the definition of Caputo derivative has been used in the system model, the definition of Riemann-Liouville will change to the definition of Caputo after taking derivatives by (3).

$$\begin{aligned} \dot{S}_S &= {}^{C}D^{\alpha_2}(S-0.1) + (S-0.1) + \frac{e_1(0)}{\Gamma(1-\alpha_2)t^{\alpha_2}} \\ \dot{S}_{DO} &= {}^{C}D^{\alpha_3}(DO-2) + (DO-2) + \frac{e_2(0)}{\Gamma(1-\alpha_3)t^{\alpha_3}} \end{aligned} \tag{17}$$

To calculate nominal controllers of related equations and certain amounts of parameters, they have been put in (18) and (19), then they are separated.

$$\begin{aligned}
&\dot{S}_S = {}^{C}D^{\alpha_2}(S-0.1)+(S-0.1)\\
&=-\frac{1}{0.67}(0.11\times\frac{S}{S+0.18}\times\frac{DO}{DO+0.2}-0.02)X\\
&-2DS+1.2D-{}^{C}D^{\alpha_2}0.1\\
&+dis1(t)+(S-0.1)=0\\
&\hat{h}_S=-\frac{1}{0.67}(0.11\times\frac{S}{S+0.18}\times\frac{DO}{DO+0.2}-0.02)X\\
&-{}^{C}D^{\alpha_2}0.1+\frac{e_1(0)}{\Gamma(1-\alpha_2)t^{\alpha_2}}+dis1(t)+(S-0.1)\\
&\hat{b}_S=(1.2-2S)\hat{D}
\end{aligned} \tag{18}$$

$$\begin{aligned}
&\dot{S}_{DO}={}^{C}D^{\alpha_3}(DO-2)+(DO-2)\\
&=(-54.1791\frac{S}{S+0.18}\times\frac{DO}{DO+0.2}+9.8507)X\\
&-2D\times DO+0.1980\times W(8-DO)+2D-\\
&{}^{C}D^{\alpha_3}2+dis2(t)+(DO-2)=0
\end{aligned}$$

$$\begin{aligned}
&\hat{h}_{DO}=(-54.1791\frac{S}{S+0.18}\times\frac{DO}{DO+0.2}+9.8507)X\\
&-{}^{C}D^{\alpha_3}2+\frac{e_2(0)}{\Gamma(1-\alpha_3)t^{\alpha_3}}+dis2(t)+(DO-2)\\
&\hat{b}_{DO}=(-2DO+2)\hat{D}+0.198(8-DO)\hat{W}
\end{aligned} \tag{19}$$

Calculations are organized in terms of a matrix.

$$\begin{aligned}
&\begin{bmatrix}\dot{S}_S\\ \dot{S}_{DO}\end{bmatrix}=\begin{bmatrix}h_s\\ h_{DO}\end{bmatrix}+\begin{bmatrix}1.2-2S & 0\\ 2-2DO & 0.198(8-DO)\end{bmatrix}\begin{bmatrix}\hat{D}\\ \hat{W}\end{bmatrix}\\
&=\hat{h}+\hat{b}\hat{u}
\end{aligned} \tag{20}$$

Where $\hat{D}$ and $\hat{W}$ are nominal controllers. Ultimate controllers are achievable in terms of equation (21).

$$u=-\hat{b}^{-1}(\hat{h}+\begin{bmatrix}k_1 sign(S_S)\\ k_2 sign(S_{DO})\end{bmatrix}) \tag{21}$$

where sign denotes the sign function. Normal sliding mode controllers are achieved as in (22) by matrix calculations mentioned above.

$$\begin{aligned}
&D=(\frac{1}{2S-1.2})[-\frac{1}{0.67}(0.11\times\frac{S}{S+0.18}\times\frac{DO}{DO+0.2}-0.02)X\\
&-D^{\alpha_2}0.1+\frac{e_1(0)}{\Gamma(1-\alpha_2)t^{\alpha_2}}+dis1(t)+S-0.1+k_1 sign(S_S)]\\
&W=(\frac{2-2DO}{0.198(DO-8)(2S-1.2)})\times\\
&[(-\frac{1}{0.67}(0.11\times\frac{S}{S+0.18}\times\frac{DO}{DO+0.2}-0.02)X\\
&-D^{\alpha_2}0.1+dis1(t)+S-0.1\\
&\frac{e_1(0)}{\Gamma(1-\alpha_2)t^{\alpha_2}}+k_1 sign(S_S)]\\
&+(\frac{1}{0.198(DO-8)})\times\\
&[(-54.1791\frac{S}{S+0.18}\times\frac{DO}{DO+0.2}+9.8507)X\\
&-D^{\alpha_3}2+dis2(t)+\\
&\frac{e_2(0)}{\Gamma(1-\alpha_3)t^{\alpha_3}}+DO-2+k_2 sign(S_{DO})]
\end{aligned} \tag{22}$$

Simulation is carried out by taking $k_1=k_2=1$. These amounts are defined in accordance with a period of changes in uncertainties and boundary of disturbances. Slight differences in parameters changes are about the hundredth. k_1 and k_2 have somehow been achieved by trial and error. The reason why they have been selected is the logical results of simulation in all states after implementing the controllers.

3.3. High-order sliding mode controllers

In order implement high-order sliding mode controllers, same previous sliding surfaces were used. First of all, virtual controllers V_D and V_W are added to the system dynamic equations.

$$C_D{}^{0.7}X = (0.11\times\frac{S}{S+0.18}\times\frac{DO}{DO+0.2}-0.02)X - 2DX - DX_r$$

$$C_D{}^{0.8}S = -\frac{1}{0.67}(0.11\times\frac{S}{S+0.18}\times\frac{DO}{DO+0.2}-0.02)X - 2DS + 1.2D + dis1(t)$$

$$D^1D = V_D$$

$$C_D{}^{0.5}DO = (-54.1791\frac{S}{S+0.18}\times\frac{DO}{DO+0.2}+9.8507)X - 2D\times DO + 0.1980\times W(8-DO) + 2D + dis2(t)$$

$$D^1W = V_W$$

$$C_D{}^{0.4}X_r = (0.0340X - 0.03X_r)D \quad (23)$$

The relative degree of the output with respect to input must be calculated to select a suitable controller. The relative degree is defined as the time derivative of output along the trajectory of the system. This is possible through Lie derivative. Therefore, an applicable definition of Lie derivative is presented for smooth functions [37].

Definition 3: if $S(x)$ is a smooth function, in the case that $x\in R^n$ and f is a smooth vector field, then the operator of Lie derivative (L) operates as in (24) with local coordination.

$$L_f S(x_1,...,x_n) = (\frac{\partial S}{\partial x_1}\cdots\frac{\partial S}{\partial x_n})\begin{pmatrix} f_1(x_1,...,x_n)\\ \vdots \\ f_n(x_1,...,x_n)\end{pmatrix} \quad (24)$$

Practically, in order to achieve a relative degree, it is possible to directly take derivative from the output; thus, the input will pop up for the first time. The number of derivative taking equals the relative degree [25] [37].

The relative degree of output S_S with respect to input V_D is achieved by the (25).

$$\dot{S}_S = {}^R D^{\alpha_2}(S-0.1) + (S-0.1) = {}^C D^{\alpha_2}(S-0.1) + (S-0.1) + \frac{e_1(0)}{\Gamma(1-\alpha_2)t^{\alpha_2}} = h_S + b_S D$$

,

$$h_S = -\frac{1}{0.67}(0.11\times\frac{S}{S+0.18}\times\frac{DO}{DO+0.2}-0.02)X - 2DS + (S-0.1) + dis1(t), b_S = 1.2-2S$$

,

$$\ddot{S}_S = \dot{h}_S + \dot{b}_S D + b_S\dot{D}$$
$$\dot{D} = V_D$$
$$\ddot{S}_S = \dot{h}_S + \dot{b}_S D + b_S V_D \quad (25)$$

So the relative degree equals 2.

The relative degree of the output S_{DO} with respect to the input V_W is also achieved by (26).

$$\dot{S}_{DO} = {}^R D^{\alpha_3}(DO-2) + (DO-2) = {}^C D^{\alpha_3}(DO-2) + (DO-2) + \frac{e_2(0)}{\Gamma(1-\alpha_3)t^{\alpha_3}} = h_{DO} + b_{DO}W + b'_{DO}D$$

,

$$h_{DO} = (-54.1791\frac{S}{S+0.18}\times\frac{DO}{DO+0.2}+9.8507)X + (DO-2) + dis2(t)$$
$$b'_{DO} = -2DO+2, b_{DO} = +0.1980(8-DO)$$
$$D^1W = V_W$$
$$\ddot{S}_{DO} = h_{DO} + \dot{b}_{DO}W + b_{DO}\dot{W} + \dot{b}'_{DO}D + b'_{DO}\dot{D}$$
$$D^1D = V_D$$
$$\ddot{S}_{DO} = \dot{h}_{DO} + \dot{b}_{DO}W + b_{DO}V_W + \dot{b}'_{DO}D + b'_{DO}V_D \quad (26)$$

According to (26), the relative degree of output in relation to both virtual controllers equals 2. Therefore, the structure of second-order sliding mode is selected.

To avoid fractional calculations in Lie derivative, the sliding surface is in the form of integrals. Otherwise, there is a possibility of a fractional relative degree appearing. Levant designed the high-order controllers for systems with integer relative degrees. So, the structure of these controllers might not be the best choice for the systems with a fractional relative degree.

A second-order sliding mode controller for the virtual input V_D is as that in (27) as following.

$$\dot{z}_0 = v_0$$
$$v_0 = -5\left|z_0 - S_S\right|^{0.5} sign(z_0 - S_S) + z_1$$
$$z_1 = -sign(z_1 - v_0)$$
$$V_D = -0.01\left(\frac{z_1 + \left|z_0\right|^{0.5} sign(z_0)}{\left|z_0\right|^{0.5} + \left|z_1\right|}\right) \quad (27)$$

Where z_0 and z_1 indicate the first and second derivative of the S_S, respectively. The variable v_0 is the robust form of z_0 as described in [25]. A second-order sliding mode controller for the virtual input V_W is as that in (28) as following.

$$\dot{\zeta}_0 = \upsilon_0$$
$$\upsilon_0 = -1\left|\zeta_0 - S_{DO}\right|^{0.5} sign(\zeta_0 - S_{DO}) + \zeta_1$$
$$\zeta_1 = -1 sign(\zeta_1 - \upsilon_0)$$
$$V_W = -10\left(\frac{\zeta_1 + \left|\zeta_0\right|^{0.5} sign(\zeta_0)}{\left|\zeta_0\right|^{0.5} + \left|\zeta_1\right|}\right) \quad (28)$$

Where ζ_0 and ζ_1 show the first and second derivative of S_{DO}, respectively. The variable υ_0 is the robust form of ζ_0. Coefficients of robust homogeneous differentiators are achieved by simulation.

4. SIMULATION AND RESULTS

The efficiency of both controllers was compared by changing uncertain parameters of the model in restricted intervals. The related results are demonstrated simultaneously. A step of simulation has been considered 0.001. Initial conditions measured as $X(0) = 0.7g.L^{-1}, S(0) = 1.2g.L^{-1}, DO(0) = 2mg.L^{-1}$ and $X_r(0) = 0.7g.L^{-1}$. In the first part, sliding surfaces are plotted.

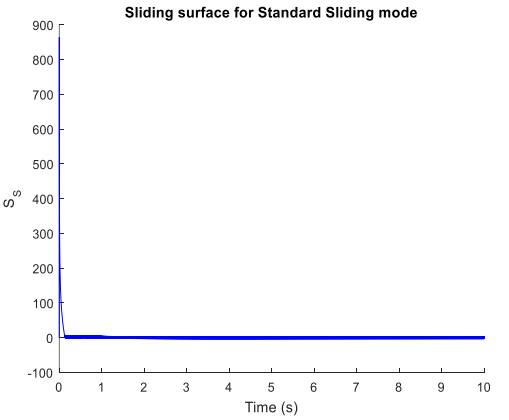

Fig. 2. Sliding surface to control S by Standard SMC.

To check the chattering amplitude precisely, the Fig. 3 is plotted. It is depicted by a reasonable limitation on a vertical axis.

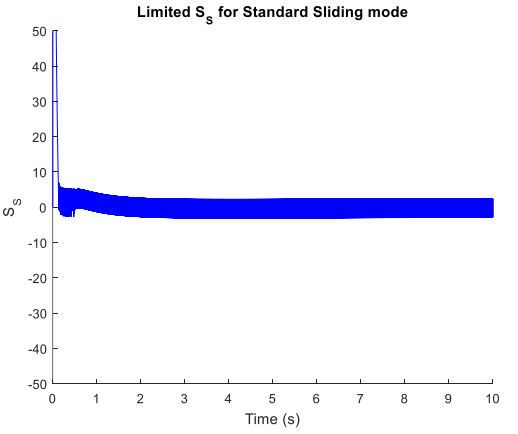

Fig. 3. Sliding Surface to control S by limitation in Y-Axis.

The amplitude of chattering is less than 10.

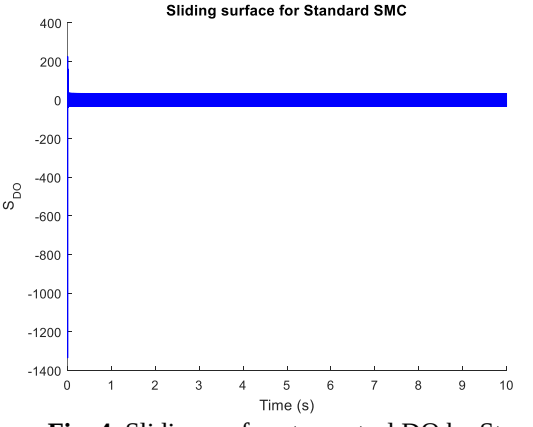

Fig. 4. Sliding surface to control DO by Standard SMC.

The chattering can be seen obviously in Fig. 4. The amplitude is about 67.

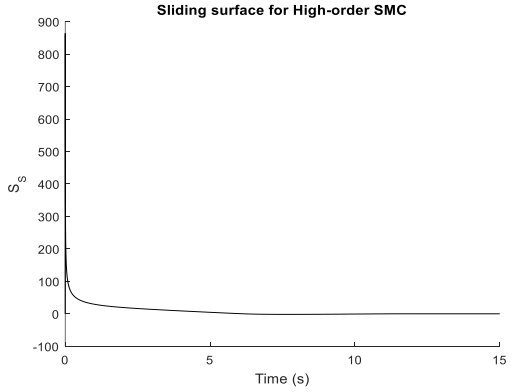

Fig. 5. Sliding surface to control S by 2nd order SMC.

The Fig. 5 is depicted for 15 seconds, to see the behavior of the sliding surface after transient time. Limiting the vertical axis leads to Fig. 6.

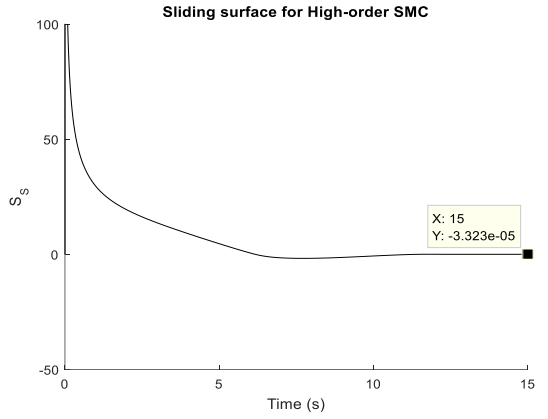

Fig. 6. Sliding surface to control *S* by 2nd order SMC.

In Fig. 6 the amplitude of chattering is about 0.00001, so it is not visible.

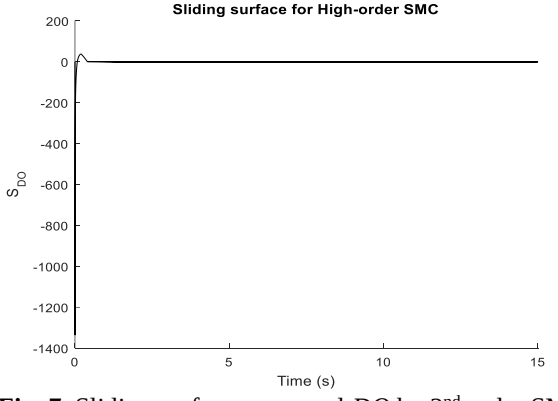

Fig. 7. Sliding surface to control *DO* by 2nd order SMC.

By limiting the vertical axis Fig. 8 is obtained.

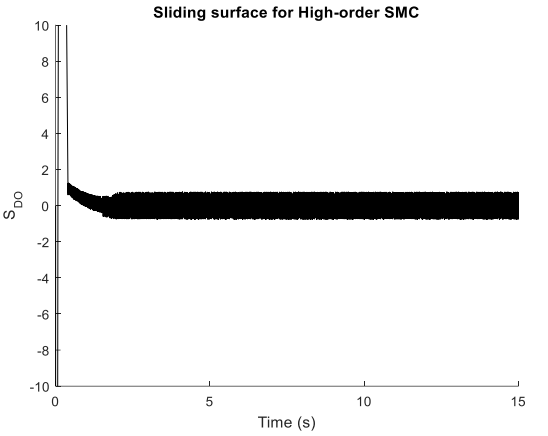

Fig. 8. Sliding surface to control *DO* by 2nd order SMC.

The Fig. 8 shows the amplitude of chattering, which is approximately 1.4. The simulation for first sliding surface shows that the chattering amplitude in standard SMC is 10^6 times greater than the high-order sliding mode controller. Also, figures of the second sliding surface show that the chattering amplitude in standard SMC is nearly 47 times greater than the high-order one.

Chattering is unintended motions with infinite frequency on sliding surfaces. These unintended motions are influential on trajectories of system and controllers. The highest chattering is seen in "Fig. 4" which has been implemented by standard sliding mode. Trajectories of outputs are depicted as follows:

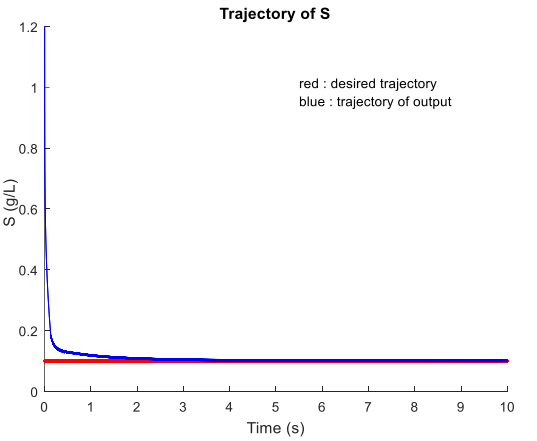

Fig. 9. Trajectory of *S* by Standard SMC.

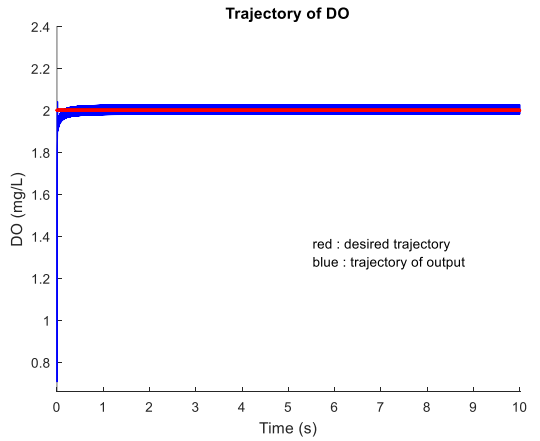

Fig. 10. Trajectory of *DO* by Standard SMC.

The simulation results in Fig. 9 and Fig. 10 show that outputs in the standard sliding mode controller track desired values in a small transient time, successfully.

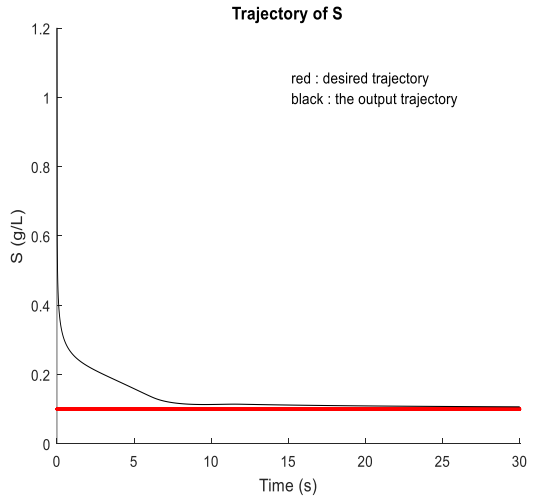

Fig. 11. Trajectory of *S* by 2nd order SMC.

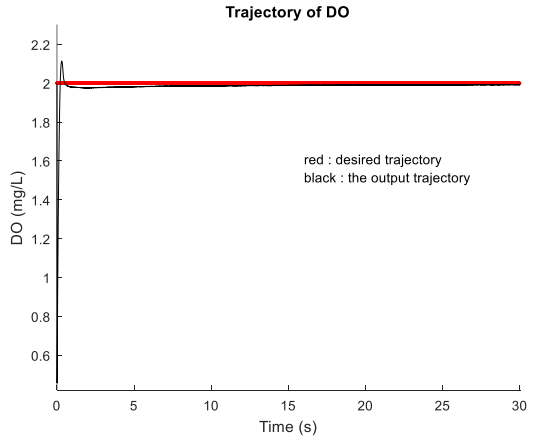

Fig. 12. Trajectory of DO by 2nd order SMC.

The simulation ran during 30 seconds, due to a longer transient time in the 2nd order sliding mode controller. According to the Fig. 11 and Fig. 12, it can be signified that outputs track the desired trajectory, successfully.

Chattering exists in all Figs because chattering is not removable thoroughly in sliding mode. In order for the controller to move on an uncertain interval, it is needed to contain a discrete structure. In the structure of both controllers, the sign function exists. The chattering affects the trajectory of outputs.

The chattering phenomenon is checked for the controller since high control activities in a controller has a destructive influence on it. High control activities cause exhaustion and can excite those neglected high frequencies in the system model, consequently.

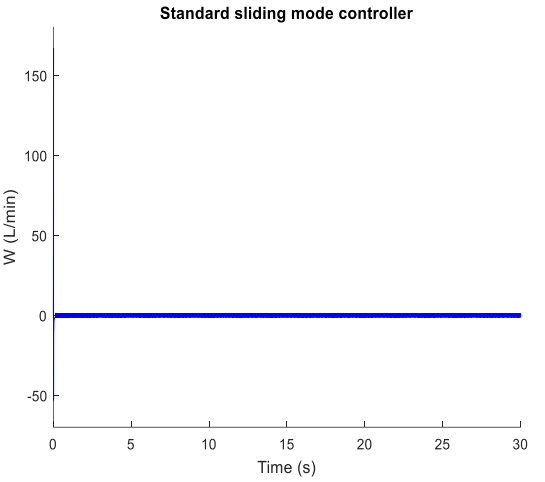

Fig. 13. *W* designed as standard sliding mode controller.

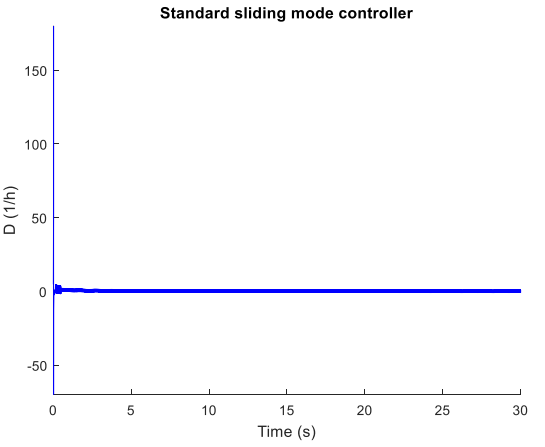

Fig. 14. *D* designed as standard sliding mode controller.

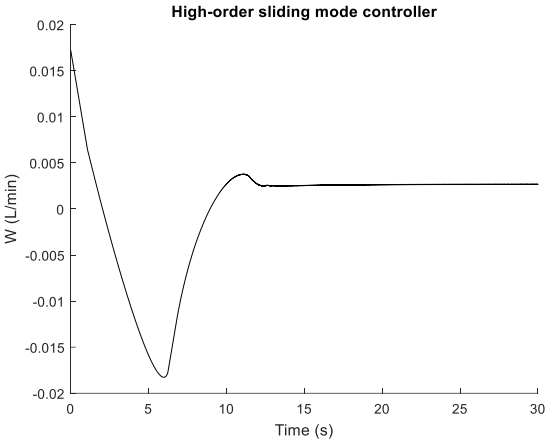

Fig. 15. *W* designed as 2nd order SMC.

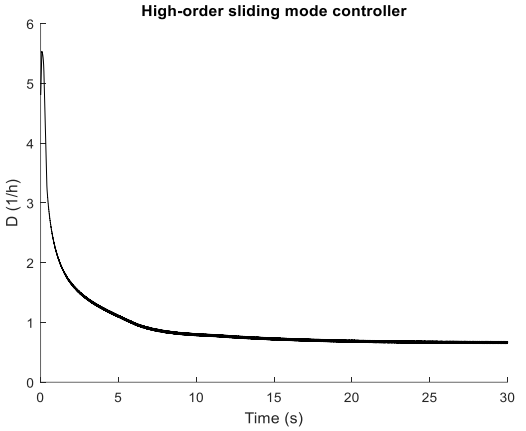

Fig. 16. *D* designed as 2nd order SMC.

To compare chattering, related figures are demonstrated at the same plots and their restrictions are implemented on a vertical axis. Blue color indicates standard sliding mode and black one signifies second-order sliding mode.

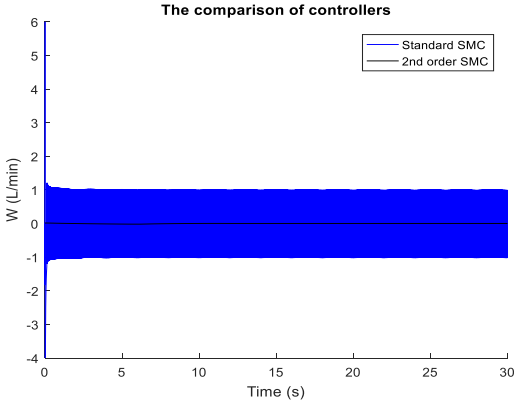

Fig. 17. Comparison of *W* designed by Standard SMC and 2nd order SMC.

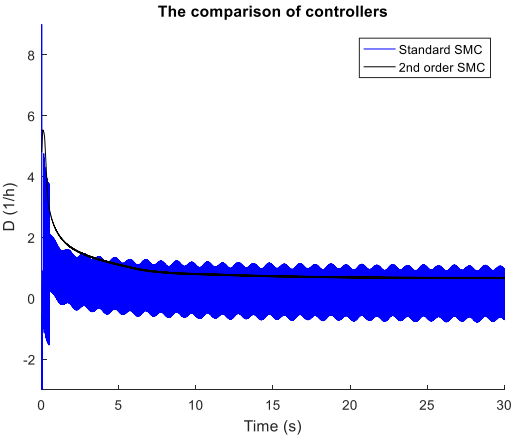

Fig. 18. The comparison of *D* designed by Standard SMC and 2nd order SMC

As seen in Figs 17 and 18, chattering amplitude in second-order sliding mode controller is too less than that of standard sliding mode.

5. CONCLUSION

Despite the presence of bounded uncertainty in the system, controllers with standard sliding mode and high-order sliding mode were designed and simulated. Both controllers used fractional order sliding surface due to the need for specific calculations. Both controllers have fractional-order type of structure because of fractional order sliding surface existing in them. Properties of fractional calculus were used in a way that we could obviate the need for direct calculations in fractional order. In order to make it possible to use the designed controllers in those including high-order sliding mode, system relative degree became an integer by taking a suitable output. To show the performance of the designed high-order controller, it was compared to a standard sliding mode controller, which confirmed the efficiency of the high-order controller. Results of the simulation also indicated that chattering is not removed in this way. Its amplitude reduces highly, though.

REFERENCES

[1] R. Hilfer, **"Applications of Fractional Calculus in Physics,"** *Singapore: World Scientific Publishing*, 2001.

[2] I. Podlubny, **"Fractional Differential Equations,"** *ACADEMIC PRESS*, 1999.

[3] N. Laskin, **"Fractional market dynamics,"** *Physica A: Statistical Mechanics and its Applications*, Vol. 287, pp. 482–492, 2000.

[4] B. Xin, T. Chena and Y. Liu, **"Projective synchronization of chaotic fractional-order energy resources demand-supply systems via linear control,"** *Communications in Nonlinear Science and Numerical Simulation*, Vol. 16, No. 11, pp. 4479–4486, 2011.

[5] R. Bagley and R. Calico, **"Fractional order state equations for the control of viscoelastically damped structures,"** *J. Guidance, Contr. & Dynamics*, Vol. 14, pp. 304–311, 1991.

[6] O. Heaviside, **"Electromagnetic Theory,"** 3rd ed. New York: Chelsea Publishing Company, 1971.

[7] A. El-Sayed, **"Fractional-order diffusion wave equation,"** *International Journal of Theoretical Physics*, Vol. 35, pp. 311–322, 1996.

[8] A. El-Misiery and E. Ahmed, **"On a fractional model for earthquakes",** *Applied Mathematics and Computation*, Vol. 178, pp. 207–211, 2006.

[9] Zhenhai Liu and Peifen Lu, **"Stability analysis for HIV infection of CD4+T-cells by a fractional differential time-delay model with cure rate,"** *Advances in Difference Equations 2014*, 2014:298.

[10] Ibrahima N'Doye, Holger Voos, Mohamed Darouach and Jochen G. Schneider, **"Static Output Feedback H∞ Control for a Fractional-order Glucose-insulin System,"** *International Journal of Control, Automation, and Systems*, Vol. 13, No. 4, pp. 1-10, 2015.

[11] Y. Tang, Y. Wang, M. Han and Q. Lian, **"Adaptive Fuzzy Fractional-Order Sliding Mode Controller Design for Antilock Braking Systems,"** *Journal of Dynamic Systems, Measurement and Control, Transactions of the ASME*, Vol. 138, No. 4, 2016.

[12] M. Rahmani, A. Ghanbari and M.M. Ettefagh, **"Robust adaptive control of a bio-inspired robot manipulator using bat algorithm,"** *Expert Systems with Applications*, Vol. 56, 164-176, 2016.

[13] A. J. Munoz-Vazquez, V. Parra-Vega, A. Sanchez-Orta, O. Garcia and C. Izaguirre-Espinoza, **"Attitude tracking control of a quadrotor based on absolutely continuous fractional integral sliding modes,"** *IEEE Conference on Control Applications*, 717-722, 2014.

[14] S. Han, Z. Jiao, C. Wang, Y. Shang and Y. Shi, **"Fractional integral sliding mode nonlinear controller of electrical-hydraulic flight simulator,"** *Beijing Hangkong Hangtian Daxue Xuebao/Journal of Beijing University of Aeronautics and Astronautics*, Vol. 40, No. 10, 1411-1416, 2014.

[15] L. Deng and S. Song, **"Flexible spacecraft attitude robust tracking control based on fractional order sliding mode,"** *Hangkong Xuebao/Acta Aeronautica et Astronautica Sinica*, Vol. 34, No. 8, August, 1915-1923, 2013.

[16] A. Biswas, S. Dasa, A. Abrahamb and S. Dasguptaa, **"Design of fractional-order $PI^{\lambda}D^{\mu}$ controllers with an improved differential evolution,"** *Engineering Applications of Artificial Intelligence*, Vol. 22, No. 2, pp. 343–350, 2009.

[17] T. Li, Y. Wang and Y. Yang, **"Designing synchronization schemes for fractional-order chaotic system via a single state fractional-order controller,"** *Optik*, Vol. 125, No. 22, pp. 6700–6705, 2014.

[18] H. S. Lafmejani and N. Bigdeli, **"Multi-Surface Sliding Mode Controller for Stabilizing Uncertain Disturbed Fractional-Order Chaotic Systems,"** *International Journal of Mechatronics, Electrical and Computer Technology*, Vol. 4, No. 11, pp. 414-429, 2014.

[19] Y. Chen, Y. Wei, H. Zhong and Y. Wang, **"Sliding mode control with a second-order switching law for a class of nonlinear fractional order systems,"** *Nonlinear Dynamics*, Vol. 85, No. 1, pp. 1-11, 2016.

[20] C. Ionescu and C. Muresan, **"Sliding Mode Control for a Class of Sub-Systems with Fractional Order Varying Trajectory Dynamics,"** *Fractional Calculus and Applied Analysis*, Vol. 18, No. 6, 1441–1451, 2015.

[21] A. Si-Ammour, S. Djennoune and M. Bettayeb, **"A sliding mode control for linear fractional systems with input and state delays,"** *Communications in Nonlinear Science and Numerical Simulation*, Vol. 14, No. 5, pp. 2310–2318, 2009.

[22] A. Levant, **"Higher order sliding: differentiation and black-box control"** in *Proceedings of the 39th IEEE Conference on Decision and Control*, 2000.

[23] A. Levant, **"Introduction to high-order sliding modes",** 2003.

[24] L. Fridman and A. Levant, **"higher order sliding modes"** in *Sliding Mode Control in Engineering*, New York: Marcel Dekker, pp. 53-101, 2002.

[25] Y. Shtessel *et al.*, **"Higher-Order Sliding Mode Controllers and Differentiators,"** in *Sliding Mode Control and Observation*, New York: Springer, 2014.

[26] A. Rhif, **"A High Order Sliding Mode Control with PID Sliding Surface: Simulation on a Torpedo,"** *International Journal of Information Technology, Control and Automation (IJITCA)*, Vol. 2, No.1, January 2012.

[27] A. Girin, F. Plestan, X. Brun and A. Glumineau**, "High-Order Sliding-Mode Controllers of an Electropneumatic Actuator: Application to an Aeronautic Benchmark,"** *IEEE Transactions on control systems technology*, Vol. 17, No. 3, May 2009.

[28] X. Liu and Y. Han, **"Finite time control for MIMO nonlinear system based on higher-order sliding mode,"** *ISA Transactions*, Vol. 53, No. 6, pp. 1838-1846, 2014.

[29] R. B. Sankar, B. Bandyopadhyay and H. Arya, **"Roll Autopilot Design of a Tactical Missile using Higher Order Sliding Mode technique,"** *2016 Indian Control Conference*, Hyderabad, India, 2016, pp. 298-303.

[30] A. Arisoy, M.K. Bayrakceken, S. Basturk, M. Gokasan and O.S. Bogosyan, **"High order sliding mode control of a space robot manipulator,"** *Recent Advances in Space Technologies (RAST) 2011 5th International Conference on*, 2011, pp. 833-838.

[31] R. Ling, Y. Dong, M. Wu and Y. Chai, **"High-Order Sliding-Mode Control for DC-DC Converters,"** *2012 IEEE 7th International Power Electronics and Motion Control Conference*, Harbin, China, 2012, pp. 1781-1786.

[32] L. Peng, M. Jianjun, G. Lina and Z. Zhiqiang, **"Adaptive Higher Order Sliding Mode Control for Uncertain MIMO Nonlinear Systems,"** *Proceedings of the 35th Chinese Control Conference*, Chengdu, China, 2016, pp. 3442-3447.

[33] A. Pisano, M. R. Rapaić, Z. D. Jeličić and E. Usai, **"On second-order sliding-mode control of fractional-order dynamics,"** *2010 American Control Conference*, Baltimore, MD, 2010, pp. 6680-6685.

[34] A. Chiroşcă, G. Ifrim, A. Filipescu and S. Caraman, **"Multivariable H_∞ Control of Wastewater Biological Treatment Processes,"** *CEAI*, Vol. 15, No.1, pp. 11-21, 2013.

[35] J.J.E. Slotine, **"Sliding Control,"** in *Applied Nonlinear Control*, New Jersey, Prentice Hall, 1991, ch. 7, sec. 7.1, pp. 285-286.

[36] B. Jakovljevic, A. Pisano, M. R. Rapai and E. Usai, **"On the sliding-mode control of fractional-order nonlinear uncertain dynamics,"** *International journal of robust and nonlinear control*, Vol. 26, pp. 782-798, 2016.

[37] F.J. Doyle and M.A. Henson, **"Nonlinear systems theory,"** in M.A. Henson and D.E. Seborg (Eds), *Nonlinear Process Control*, Prentice Hall, 1997.